Spin-dependent electron transport in a Rashba quantum wire with rough edges

Xianbo Xiao[1,2], Huili Li[1], Guanghui Zhou[3] and Nianhua Liu[2†]

[1] School of Computer, Jiangxi University of Traditional Chinese Medicine, Nanchang 330004, China.

[2] Institute for Advanced Study, Nanchang University, Nanchang 330031, China.

[3] Department of Physics, Hunan Normal University, Changsha 410081, China.

E-mail: nhliu@ncu.edu.cn

Abstract. We investigate theoretically the spin-dependent electron transport in a Rashba quantum wire with rough edges. The charge and spin conductances are calculated as function of the electron energy or the wire length by adopting the spin-resolved lattice Green function method. For a single disordered Rashba wire, it is found that the charge conductance quantization is destroyed by the edge disorder. However, a nonzero spin conductance can be generated and its amplitude can be manipulated by the wire length, which is attributed to the broken structure symmetries and the spin-dependent quantum interference induced by the rough boundaries. For a large ensemble of disordered Rashba wires, the average charge conductance decreases monotonically, however, the average spin conductance increases to a maximum value and then decreases, with increasing wire length. Further study shows that the influence of the rough edges on the charge and spin conductances can be eliminated by applying a perpendicular magnetic field to the wire. In addition, a very large magnitude of the spin conductance can be achieved when the electron energy lies between the two thresholds of each pair of subbands. These findings may not only benefit to further apprehend the transport properties of the Rashba low-dimensional systems but also provide some theoretical instructions to the application of spintronics devices.

† Author to whom any correspondence should be addressed.

1. Introduction

In 1990, Datta and Das proposed a novel device, i.e. spin-field-effect transistor [1], which demonstrates that the spin state of the conduction electrons in a quasi-two-dimensional electron gas (2DEG) can be controlled via the Rashba spin-orbit interaction (SOI) [2, 3]. From then on, the spin-dependent electron transport in low-dimensional semiconductor quantum systems under the modulation of Rashba SOI has drawn intensive investigation [4], since it is the physical basis of semiconductor spintronics devices. In these devices, the spin instead of charge degree of freedom of the conduction electrons is utilized to store and communicate information.

Modern nanofabrication techniques allow the manufacture of various high quality low-dimensional quantum structures, however, the disorders such as impurities, defects and rough edges are inevitable in these systems[5]. Therefore, the effects of these disorders on the spin-dependent electron transport should be considered in the application of semiconductor spintronics devices. In previous works, the influence of the scattering caused by the impurities and defects on the function of the semiconductor spintronics devices such as spin filter [6, 7, 8, 9, 10], spin transistor [11, 12], spin diode [13] and spin separator [14] has been studied extensively. Furthermore, the impurity and defect disorders also result in the strength of the SOI to fluctuate randomly in space, leading to many new phenomena such as the realization of the minimum possible strength of SOI [15] and the localization of the edge electrons for sufficiently strong electron-electron interactions [16]. However, recent studies show that the scattering induced by the impurities and defects has the same impact on every propagating channel in low-dimensional quantum structures while the scattering caused by the rough edges mainly impact the highest propagating channel [17, 18, 19, 20, 21, 22]. Thereby, the edge disorder may give rise to some new effects in the spin-dependent electron transport of the low-dimensional quantum systems under the modulation of the Rashba SOI. To the best of our knowledge, the effects of the edge disorder on the spin-dependent electron transport have not yet been investigated up to now.

In order to uncover the novel transport phenomena induced by the rough edges in low-dimensional quantum structures, in this paper we theoretically calculate the charge and spin conductances at low temperatures for a Rashba quantum wire in the presence of the edge disorder. It is demonstrated that the spin conductance displays very different behaviors compared to those of the charge conductance when spin-unpolarized electrons are injected from the input lead. The quantum charge conductance steps for a single disordered Rashba wire are destroyed and decreases dramatically with increasing wire length, that is, edge disorder strength. However, a spin-polarized current can be generated in the output lead and its magnitude is very sensitive to the wire length. Similarly, the average charge conductance for a large ensemble of disordered Rashba wires are suppressed gradually while the average spin conductance are enhanced firstly and then suppressed, with the increasing of the wire length. Further study shows that the edge disorder effects on the spin-dependent electron transport can be removed when

a perpendicular magnetic field is applied to the quantum wire. The quantum charge conductance steps recover one by one with an increase of the magnetic field strength. However, the spin conductance almost disappears except within the energy window between the two thresholds of each pair of subbands, where a very large amplitude of spin conductance can be obtained.

The rest of the paper is organized as follows. In section 2, the theoretical model and the spin-resolved lattice Green function approach are presented. Some numerical examples and discussions of the results are demonstrated in section 3. Finally, section 4 concludes the paper.

2. Model and Method

The system studied in present work is schematically depicted in figure 1, where a 2DEG in the (x, y) plane is restricted to a quantum wire with rough edges by a confining potential $V(x, y)$. The 2DEG is confined in an asymmetric quantum well, where the SOI is assumed to arise dominantly from the Rashba mechanism. The quantum wire has a length L and a width $W(x)$ randomly fluctuating with x, connected to two ballistic semi-infinite leads of constant width W. The two connecting leads are normal-conductor electrodes without SOI, since the spin-unpolarized injection is interested. Such kind of Rashba system can be described by the discrete lattice model. The spin-resolved tight-binding Hamiltonian including the Rashba SOI on a two-dimensional lattice is given as follows [23],

$$H = H_0 + H_{so} + V, \tag{1}$$

where

$$\begin{aligned} H_0 = &\sum_{lm\sigma} \varepsilon_{lm\sigma} c^\dagger_{lm\sigma} c_{lm\sigma} - t \sum_{lm\sigma} \{c^\dagger_{l+1m\sigma} c_{lm\sigma} \\ &+ c^\dagger_{lm+1\sigma} c_{lm\sigma} + H.c\}, \end{aligned} \tag{2}$$

$$\begin{aligned} H_{so} = t_{so} &\sum_{lm\sigma\sigma'} \{c^\dagger_{l+1m\sigma} (i\sigma_y)_{\sigma\sigma'} c_{lm\sigma'} \\ &- c^\dagger_{lm+1\sigma} (i\sigma_x)_{\sigma\sigma'} c_{lm\sigma'} + H.c\}, \end{aligned} \tag{3}$$

and

$$V = \sum_{lm\sigma} v_{lm} c^\dagger_{lm\sigma} c_{lm\sigma}, \tag{4}$$

in which $c^\dagger_{lm\sigma}(c_{lm\sigma})$ is the creation (annihilation) operator of electron at site (lm) with spin σ, $\sigma_{x(y)}$ is Pauli matrix, and $\varepsilon_{lm\sigma} = 4t$ is the on-site energy with the hopping energy $t = \hbar^2/2m^*a^2$, here m^* and a are the effective mass of electron and lattice constant, respectively. v_{lm} is the additional confining potential. The SOI strength is $t_{so} = \alpha/2a$ with the Rashba constant α. When a magnetic field $\vec{B}(0, 0, 1)$ is introduced, it could be incorporated into the nearest-neighbor hopping energy by the Peierl's phase factor such as

$$T_{lm,lm+1} = texp(i\hbar\omega_c l/2t) = (T_{lm+1,lm})^*; \quad T_{lm,l+1m} = (T_{l+1m,lm})^* = t, \tag{5}$$

where $\omega_c = eB/m^*c$ is the cyclotron frequency. In order to keep the transitional symmetry of system along the x-axis direction, the vector potential is chosen as $\vec{A} = (By, 0, 0)$. The SOI strength t_{so} should be given the same modification as that of the hopping energy when the magnetic field is presented. Moreover, the Zeeman effect from the external magnetic field is not included here.

In order to calculate the Green function of the whole system through the recursive Green function method, the tight-binding Hamiltonian (1) is divided into two parts in the column cell

$$H = \sum_{l\sigma\sigma'} H_l^{\sigma\sigma'} + \sum_{l\sigma\sigma'} (H_{l,l+1}^{\sigma\sigma'} + H_{l+1,l}^{\sigma'\sigma}), \tag{6}$$

where $H_l^{\sigma\sigma'}$ is the Hamiltonian of the lth isolated column cell, $H_{l,l+1}^{\sigma\sigma'}$ and $H_{l+1,l}^{\sigma'\sigma}$ are intercell Hamiltonian between the lth column cell and the $(l+1)$th column cell with $H_{l,l+1}^{\sigma\sigma'} = (H_{l+1,l}^{\sigma'\sigma})^\dagger$, here the lattice position parameter l is within the range $[1, N]$. The Green function of the whole system can be computed by a set of recursive formulas [24, 25],

$$\langle l+1|G_{l+1}|l+1\rangle^{-1} = E - H_{l+1} - H_{l+1,l}\langle l|G_l|l\rangle H_{l,l+1}, H_{l+1,l}\langle l|G_l|0\rangle, \tag{7}$$

$$\langle l+1|G_{l+1}|0\rangle = \langle l+1|G_{l+1}|l+1\rangle H_{l+1,l}\langle l|G_l|0\rangle, \tag{8}$$

in which $\langle l|G_l|l\rangle$ and $\langle l|G_l|0\rangle$ are respectively the diagonal and off-diagonal Green function, and

$$H_{l+1} = \begin{pmatrix} H_{l+1}^{\sigma\sigma} & H_{l+1}^{\sigma\sigma'} \\ H_{l+1}^{\sigma'\sigma} & H_{l+1}^{\sigma'\sigma'} \end{pmatrix}, \quad H_{l+1,l} = (H_{l,l+1})^\dagger = \begin{pmatrix} H_{l+1,l}^{\sigma\sigma} & H_{l+1,l}^{\sigma\sigma'} \\ H_{l+1,l}^{\sigma'\sigma} & H_{l+1,l}^{\sigma'\sigma'} \end{pmatrix}. \tag{9}$$

The recursion starts from the Green function of the left semi-infinite lead without SOI $\langle 0|G_0|0\rangle$. By utilizing equation (7), the following sequences of the diagonal Green function $\langle 0|G_0|0\rangle \to \langle 1|G_1|1\rangle \to \cdots \to \langle N|G_N|N\rangle$ can be obtained. Substituting these diagonal Green functions into equation (8), the off-diagonal Green functions $\langle 1|G_1|0\rangle \to \langle 2|G_2|0\rangle \to \cdots \to \langle N|G_N|0\rangle$ can be achieved in turn. In the final recursion step, the Green function of the right semi-infinite with a vanishing SOI $\langle N+1|G_{N+1}|N+1\rangle$ is attached, and then the Green function of the whole system $\langle N+1|G_{N+1}|0\rangle$ is generated finally. Here the Green function of the left and right semi-infinite leads can be obtained analytically from reference [26].

Utilizing the Green function of the whole system calculated above, one can compute the two-terminal spin-resolved conductance through the Landauer-B$\ddot{u}$ttiker formula [27]

$$G^{\sigma'\sigma} = e^2/hTr[\Gamma_L^\sigma G^r \Gamma_R^{\sigma'} G^a], \tag{10}$$

where $\Gamma_{L(R)} = i[\sum_{L(R)}^r - \sum_{L(R)}^a]$ with the self-energy from the left (right) lead $\sum_{L(R)}^r = (\sum_{L(R)}^a)^*$, the trace is over the spatial and spin degrees of freedom, and $G^r(G^a)$ is the retarded (advanced) Green function of the whole system and $G^a = (G^r)^\dagger$.

In the following calculations, all the energy and lengths are normalized by the hopping energy $t(t=1)$ and the lattice constant $a(a=1)$, respectively. The z-axis is chosen as the spin-quantized axis so that $|\uparrow>= (1,0)^T$ represents the spin-up state and

$|\downarrow>= (0,1)^T$ denotes the spin-down state, where T means transposition. The width of the two semi-infinite leads is fixed at $W = 20$, the average value of the width of the Rashba quantum wire with rough boundaries is taken to be $\langle W(x)\rangle = 17$, i.e., $W(x)$ oscillating randomly within the range from 14 to 20. The strength of SOI is set at $t_{so} = 0.08$. For simplicity, the hard-wall confining potential approximation is adopted to determine the boundaries of the quantum wire, due to different confining potentials only alter the positions of the subbands and the energy gaps between them.

For a single disordered Rashba wire, the charge conductance and the amplitude of the spin conductance of z-component are defined as $G^e = G^{\uparrow\uparrow} + G^{\uparrow\downarrow} + G^{\downarrow\downarrow} + G^{\downarrow\uparrow}$ and $G^{Sz} = \frac{e}{4\pi}|\frac{G^{\uparrow\uparrow}+G^{\uparrow\downarrow}-G^{\downarrow\downarrow}-G^{\downarrow\uparrow}}{e^2/h}|$, respectively. Here the charge conductance means the transfer probability of electrons, and the spin conductance represents the change in local spin density between the input lead and the output lead caused by the transport of spin-polarized electrons [28]. In addition, the equation that is usually used for calculation of the localization length [29] is modified to $\lambda = -1/\lim\limits_{L\to\infty}\frac{1}{L}Tr|G^aG^r|$ as the spin degree of freedom is included.

For a large number of disordered Rashba wires, the average charge conductance and the charge conductance fluctuation are respectively quantified as $G_a^e = \langle G^e\rangle$ and $G_f^e = [\langle (G^e)^2\rangle - \langle G^e\rangle^2]^{\frac{1}{2}}$, where $\langle\cdots\rangle$ denotes averaging over an ensemble of samples with different realizations of edge disorder [30]. Similarly, we define the average spin conductance and the spin conductance fluctuations as $G_a^{Sz} = \langle G^{Sz}\rangle$ and $G_f^{Sz} = [\langle (G^{Sz})^2\rangle - \langle G^{Sz}\rangle^2]^{\frac{1}{2}}$, respectively.

3. Results and discussions

3.1. The conductance for a single Rashba quantum wire with rough edges

Figure 2(a) shows the charge conductance as function of the electron energy E for various wire lengths. By comparing with the charge conductance G^e of the ideal straight Rashba wire $W(x) \equiv 17$ (dotted line), the step structures of the charge conductance are deteriorated and its magnitude decreases dramatically within the whole energy band range even for a very small edge disorder strength $L = 10$ (dash-dotted line). The charge conductance curve also shows sample specific fluctuations, resulting from the quantum interference effect induced by the rough edges. The typical spacing between peaks and valleys in the charge conductance depends on the wire length as $E_c \sim 1/L$ [30]. Consequently, the charge conductance fluctuates quickly as the wire length L is increased to 40 (dashed line). When the wire length is increased further to 200, plenty of resonant peaks appear in the charge conductance, with the maximum value $2e^2/h$ (solid line). In addition, the charge conductance falls faster near the right energy band edge than that near the energy band center though there are more propagating channels, which can be understood by the localization length λ plotted in figure 2(c). Due to the localization lengths near the band center are larger than those near the band edges to the right, the charge conductance near the band center is subjected to less impacts of the

edge disorder. Figure 2(b) plots the amplitude of the spin conductance of z-component as function of the electron energy for the same Rashba quantum wire with rough edges. Surprisingly, the spin conductance G^{Sz} exhibits very different transmission behaviors from those of the charge conductance. Owing to the longitudinally symmetry of the straight Rashba quantum wire [31], the amplitude of the spin conductance keeps zero for the whole energy band (dotted line). However, for the Rashba wire with boundary roughness ($L = 10$), a nonzero spin conductance is generated (dash-dotted line) and its maximum amplitude is enlarged when the wire length is increased to 40 (dashed line). When the wire length is increased further to the strong localization regime $L = 200$ ($L > \lambda$), the amplitude of the spin conductance also shows plenty of resonant peaks, but the maximum value is smaller than e^2/h (solid line). The mechanism of the edge-disorder-induced spin conductance is attributed to the broken longitudinal symmetry of the Rashba wire [13, 32] and the spin-dependent quantum interference between the forward propagating channels and the backward propagating channels caused by the rough boundaries. Furthermore, due to the scattering by the rough edges is weakest in the lowest propagating channel and strongest in the highest propagating channel [17, 18, 19, 20, 21, 22], the spin-dependent quantum interference mainly happens in the highest propagating channel. As a consequence, the amplitude of the spin conductance is not larger than e^2/h.

According to figure 2, it is understood that the charge and spin conductances are very sensitive to the length of the Rashba quantum wire. In order to clarify the contribution of the wire length, the charge and spin conductances as function of the wire length are plotted in figures 3(a) and 3(b), respectively. The electron energy $E = 2.08$. It is found that the sensitivity of the charge and spin conductances to the wire length differs from that to the electron energy. As shown in figure 3(a), the charge conductance decreases sharply with the raising of the wire length if only it is smaller than the localization length $\lambda = 140$ (see figure 2(c)). However, when the wire length is increased to the strong localization regime ($140 < L \leq 300$), the charge conductance is of order $2e^2/h$ and fluctuates more obviously. As the wire length is further increased ($L > 300$), the charge conductance almost disappears in virtue of the strong backscattering caused by the edge disorder. In contrast with the charge conductance, the amplitude of the spin conductance oscillates quickly with an increase of the wire length, as shown in figure 3(b). There are many peaks and valleys exist in the spin conductance and the maximum value of these peaks almost reaches e^2/h when the wire length is increased to the strong localization region. Further, the amplitude of the spin conductance becomes very small as the wire length $L > 300$, since the charge conductance almost decreases to zero.

3.2. The average conductance and the conductance fluctuations for a large ensemble of Rashba quantum wires with rough edges

Figure 4(a) shows the ensemble average charge conductance as function of the electron energy for various wire lengths. For the short Rashba wires $L = 10$, the average charge conductance G_a^e increases sharply with the raising of the electron energy except for a short plateau of the first propagating channel, indicating that the edge disorder has less impacts for the lower propagating channel (longer wavelength). However, for the longer Rashba wire, the average charge conductance increases slowly with increasing electron energy ($L = 40$) or is independent of the electron energy within a wide range ($L = 200$). In addition, there is a broad charge conductance peak near the band edge to the left, which corresponds to peak in the localization length plotted in figure 2(c). The corresponding ensemble average spin conductance as function of the electron energy is illustrated in figure 4(b). By comparing to the average charge conductance, the average spin conductance G_a^{Sz} displays converse behaviors. The average spin conductance is almost independent of the electron energy near the band center for the short Rashba wire $L = 10$, however, it depends on the electron energy for the longer Rashba wire $L = 40$ and its magnitude is increased. Especially, when the wire length locates within the strong localization regime ($L = 200$), the average spin conductance is very sensitive to the electron energy and behaves like the localization length shown in figure 2(c). Figure 4(c) shows the charge conductance fluctuation as function of the electron energy. For the case $L = 10$, the charge conductance fluctuation G_f^e increases monotonously with the increasing of the electron energy except a broad peak appears near the band edge to the left, which corresponds to the peak in the density of states (see reference [33]). However, the charge conductance fluctuation for the case $L = 40$ increases slowly with an increase of the electron energy and its magnitude is very close to the universal value of the charge conductance fluctuation $0.729e^2/h$ [34]. Interestingly, the charge conductance fluctuation remains a constant value $0.5e^2/h$ in a wide regime of the electron energy for the case $L = 200$. The spin conductance fluctuation as function of the electron energy is plotted in figure 4(d). It is shown that the spin conductance fluctuation G_f^{Sz} has the same sensitivity to the electron energy as that of the average spin conductance G_a^{Sz}.

The ensemble average charge and spin conductances as function of the wire length are illustrated in figures 5(a) and 5(b), respectively. The electron energy E is fixed at 2.08. The average charge conductance G_a^e decreases sharply when the wire length is smaller than the localization length $\lambda = 140$. As the length of the wire is increased further, the average charge conductance decreases slowly. Conversely, when the wire length $L < 140$, the average spin conductance G_a^{Sz} increases sharply with increasing wire length and reach the maximum value $0.135e/4\pi$, indicating that the spin conductance comes from the spin-dependent interference effect. However, the average spin conductance decreases slowly as the wire length is increased further, since the charge conductance in this regime is contributed by the resonance tunneling [35] or "necklace" states [36]. Figures 5(c) and 5(d) plot the charge and spin conductance fluctuations as

function of the wire length, respectively. The charge conductance fluctuation G_f^e also decreases sharply with an increase of the wire length except at $L = 3$, where a peak emerges. However, a constant value of the charge conductance fluctuation $0.5e^2/h$ is found when the wire length is longer than the localization length $\lambda = 140$. The spin conductance fluctuation G_f^{Sz} shows the same sensitivity to the wire length as that of the average spin conductance G_a^{Sz}.

3.3. The conductance for a single Rashba wire with rough edges irradiated by a magnetic field

Figures 6(a)-(c) show the charge conductance as function of the electron energy for various magnetic field strengths. The strength of the magnetic field in each panel is taken to be $\hbar\omega_c = 0, 0.5, 1.0$, respectively. The length of the Rashba quantum wire is fixed at $L = 40$. Many resonant peaks and valleys exist in the charge conductance of the Rashba wire without magnetic field, as shown in figure 6(a), resulting from the quantum interference between the forward propagating channels and the backward propagating channels caused by the rough boundaries. However, those resonant conductance peaks and valleys are smeared and the quantum charge conductance recover step by step with the increasing of the magnetic field strength, as shown in figures 6(b) and 6(c). These effects can be apprehended by the corresponding energy band for the Rashba wire with the smallest width $W(x) = 14$ shown in the inset of each figure, which determines the charge conductance of the whole system. Each pair of the energy subbands are lifted and the energy gap between two adjacent pair of subbands is enlarged dramatically when the magnetic field strength is increased, basically equaling $\hbar\omega_c$. Thus, the quantum interference induced by the edge roughness is reduced, restoring the quantum charge conductance. The corresponding spin conductance as function of the electron energy for each magnetic field strength is plotted in figures 6(d)-(f), respectively. Interestingly, the spin conductance disappears gradually with an increase of the magnetic field strength. However, a very large magnitude of the spin conductance ($\sim e^2/h$) can be achieved between the two thresholds of each pair of subbands, i.e., a energy window with a large spin conductance is opened. Further, the width of the energy window increases with the raising of the subbands. These phenomena can also be understood by the energy band shown in each inset of figures 6(a)-(c). Due to the energy gaps between two adjacent pair of subbands are enlarged by the magnetic field, the Rashba subbands intermixing becomes negligible [37] and the spin-dependent quantum interference cause by the rough edges is reduced, resulting in the disappearance of the spin conductance. In addition, the Rashba SOI will lead to a Zeeman-like energy-band split when the perpendicular magnetic field is placed to the Rashba wire and its energy difference is $\Delta\varepsilon = (2\alpha\sqrt{2m^*}/\hbar)\sqrt{\hbar\omega_c(n+1)}$ [23], where n denotes the index of the subband. Consequently, the magnitude of the spin conductance inside the energy windows is very large and the width of the energy window increases with the raise of the subbands.

4. Summary and conclusion

In summary, we have clarified the spin-dependent electron transport properties of a Rashba quantum wire with rough boundaries attached two normal leads, and found that (i) a spin conductance can be generated due to the broken structure symmetries and the spin-dependent quantum interference caused by the rough edges; (ii) the magnitude of the spin conductance will be enhanced firstly, and then suppressed as the wire length is increased; (iii) the influence of the rouge edges on the charge and spin conductances can be eliminated when a perpendicular magnetic field is added to the Rashba quantum wire. However, a very large amplitude of the spin conductance can be generated when the electron energy is located between the two thresholds of each pair of subbands. These interesting findings may not only be useful in further understanding the spin-dependent electron transport in low-dimensional Rashba quantum structures but also provide some theoretical instructions in the preparation of spintronics devices.

Acknowledgments

This work was supported by the National Natural Science Foundation of China (Grant No. 11147156, 10832005 and 10974052), and by the Research Foundation of Jiangxi Education Department (Grant No. GJJ12532).

References

[1] Datta S and Sarma S Das 1990 *Appl. Phys. Lett.* **56** 665
[2] Rashba E I 1960 *Sov. Phys. Solid State* **2** 1109
[3] Bychkov Y A and Rashba E I 1984 *J. Phys. C* **17** 6039.
[4] Zutic I, Fabian J and Sarma S D 2004 *Rev. Mod. Phys.* **76** 323
[5] Saminadayar L, Bäuerle C and Mailly D 2004 *Encyclopedia of Nanoscience and Nanotechnology*, edited by Nalwa (American Scientific, Valencia, CA) **3** 267-285
[6] Shi Q W, Zhou J and Wu M W 2004 *Appl. Phys. Lett.* **85** 2547
[7] Yamamoto M, Ohtsuki T and Kramer B 2005 *Phys. Rev. B* **72** 115321
[8] Ohe J, Yamamoto M, Ohtsuki T and Nitta J 2005 *Phys. Rev. B* **72** 041308(R)
[9] Rebei J and Heinonen O 2006 *Phys. Rev. B* **73** 153306
[10] Yamamoto M and Kramer B 2008 *J. Appl. Phys* **103** 123703
[11] Wang L, Shen K, Cho S Y and Wu M W 2008 *J. Appl. Phys* **104** 123709
[12] Shen K and Wu M W 2008 *Phys. Rev. B* **77** 193305
[13] Xiao X B and Chen Y G 2010 *Europhys. Lett.* **90** 47004
[14] Xiao X B and Chen Y G 2010 *J. Appl. Phys* **108** 093717
[15] Sherman E Y 2003 *Phys. Rev. B* **67** 161303(R)
[16] Ström A, Johannesson H and Japaridze G I 2010 *Phys. Rev. Lett.* **104** 256804
[17] García-Martín A, Torres J A, Sáenz J J and Nieto-Vesperinas M 1998 *Phys. Rev. Lett* **80** 4165
[18] Sánchez-Gil J A, Freiliker V, Maradudin A A and Yurkevich I V 1999 *Phys. Rev. B* **59** 5915
[19] García-Martín A and Sáenz J J 2001 *Phys. Rev. Lett* **87** 116603
[20] Markoš 2006 *Acta Physica Slovaca* **56** 651
[21] Froufe-Pérez L S, Yépez M, Melo P M and Sáenz J J 2007 *Phys. Rev. E* **75** 031113
[22] Feilhauer J and Moško M 2011 *Phys. Rev. B* **83** 245328
[23] Wang J, Sun H B and Xing D Y 2004 *Phys. Rev. B* **69** 085304

[24] Lee P A and Fisher D S 1981 *Phys. Rev. Lett.* **47** 882
[25] Ando T 1991 *Phys. Rev. B* **44** 8017; Clennan M J, Lee Y and Datta S 1991 *Phys. Rev. B* **43** 13846; Baranger H U, Divincenzo D P, Jalaber R A and Stone A D 1991 *Phys. Rev. B* **44** 10637
[26] MacKinnon A 1985 *Z. Phys. B* **59** 385
[27] Büttiker M 1986 *Phys. Rev. Lett.* **57** 1761
[28] Khomitsky D V 2009 *Phys. Rev. B* **79** 205401
[29] Nikolić K and MacKinnon A 1992 *Phys. Rev. B* **47** 6555
[30] Nikolić K and MacKinnon A 1994 *Phys. Rev. B* **50** 11008
[31] Zhang Z Y 2007 *J. Phys: Condens. Matter* **19** 016209
[32] Zhai F and Xu H Q 2007 *Phys. Rev. B* **76** 035306
[33] Nikolić K and MacKinnon A 1993 *Phys. Rev. B* **47** 6555
[34] Lee P A and Stone A D 1985 *Phys. Rev. Lett.* **55** 1622; Lee P A, Stone A D and Fukuyama H 1987 *Phys. Rev. B* **35** 1039
[35] Bryant G W 1991 *Phys. Rev. B* **44** 12837
[36] Pendry J B 1987 *J. Phys. C* **20** 733
[37] Mireles F and Kirczenow G 2001 *Phys. Rev. B* **64** 024426

Figure captions

Figure 1. (a) Schematic diagram of the Rashba quantum wire with rough edges, connected to two ideal semi-infinite leads with a vanishing SOI. The two leads have the same width W. The wire has length L and width $W(x)$, randomly fluctuating with x.

Figure 2. (Color online) (a) The calculated charge conductance as function of the electron energy of a single sample of disordered Rashba quantum wire with length: $L = 10, 40$ and 200. The dotted line shows the charge conductance of a perfect Rashba wire of the width $W(x) \equiv 17$, length $L = 10$, and leads $W = 17$. (b) The amplitude of the spin conductance as function of the electron energy for the same wires. (c) The localization length for the Rashba wire with boundary roughness. Graphs in (b) are vertically offset for 2.0.

Figure 3. (a) The calculated charge conductance as function of the wire length of a single sample of disordered Rashba quantum wire. (b) The amplitude of the spin conductance as function of the wire length for the same wire. The electron energy $E = 2.08$.

Figure 4. (Color online) The average charge (a) and spin (b) conductances as function of the electron energy for different wire lengths: $L = 10, 40$ and 200. The charge (c) and spin (d) conductance fluctuations corresponding to the case in (a) and (b), respectively. Number of samples taken for calculating average and fluctuations value is 1000.

Figure 5. The average charge (a) and spin (b) conductances as function of the wire length for the electron energy $E = 2.08$. The charge (c) and spin (d) conductance fluctuations corresponding to the case in (a) and (b), respectively. Number of samples taken for calculation is the same as that in figure 4.

Figure 6. (Color online) (a)-(c) The charge conductance as function of the electron energy of a single disordered Rashba quantum wire for different magnetic field strengths: $\hbar\omega_c = 0, 0.5$, and 1.0. The inset in each panel is the energy band of a straight Rashba wire with width $W(x) = 14$, placed in a perpendicular magnetic field. (d)-(f) The amplitude of the spin conductance as function of the electron energy. The wire length is set at $L = 40$.

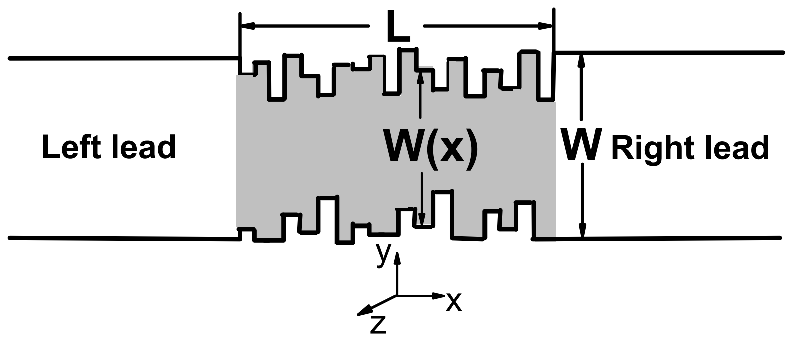

Figure 1

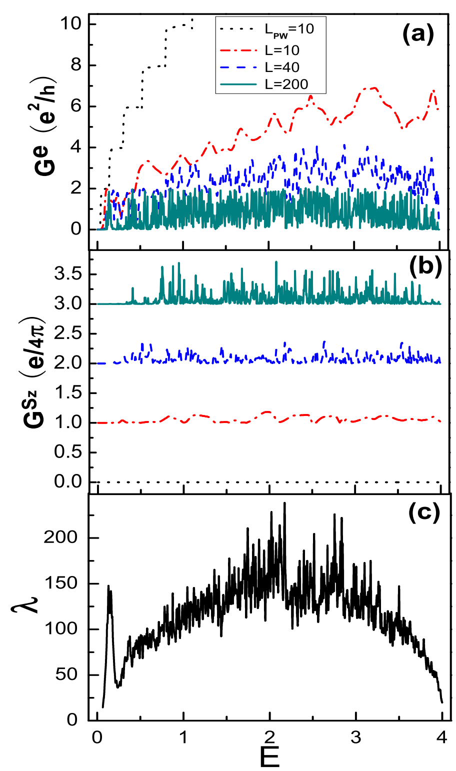

Figure 2

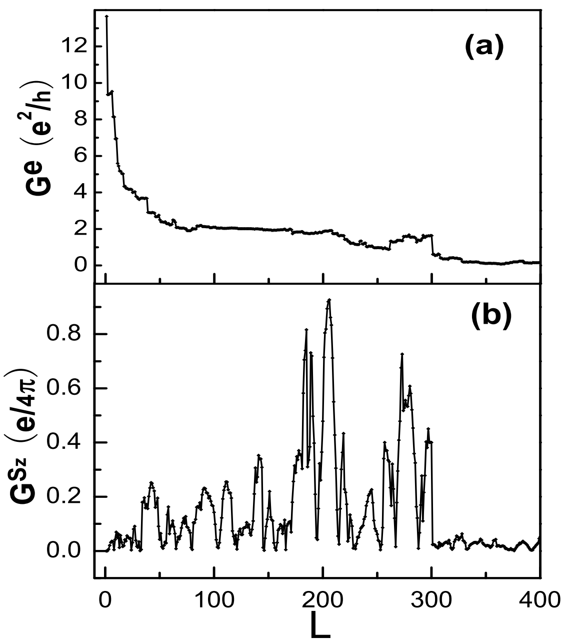

Figure 3

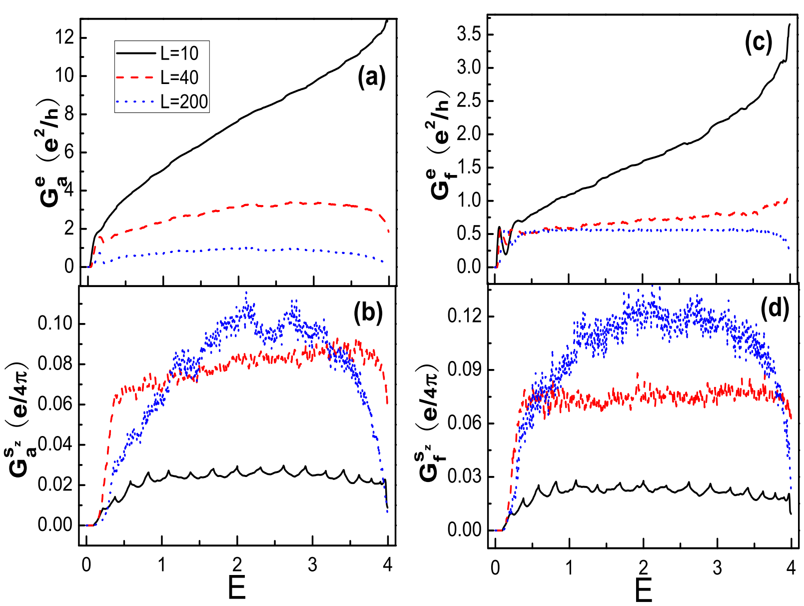

Figure 4

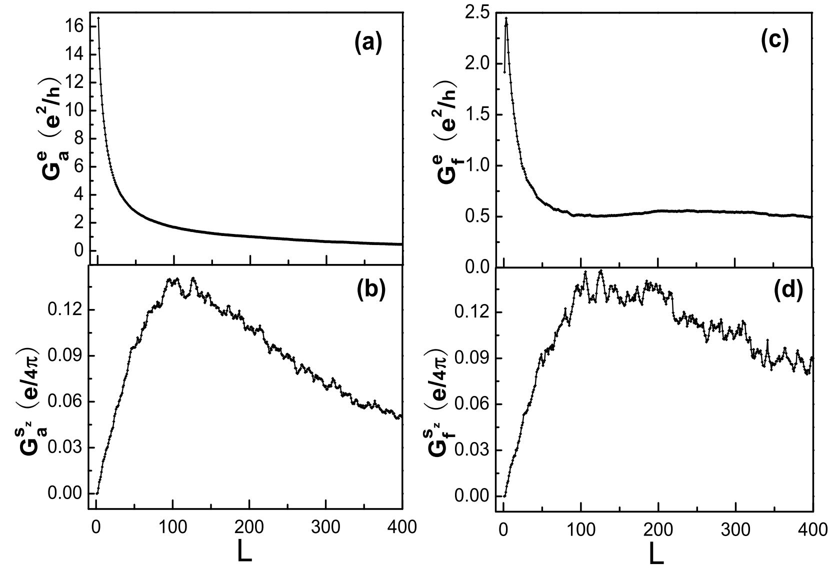

Figure 5

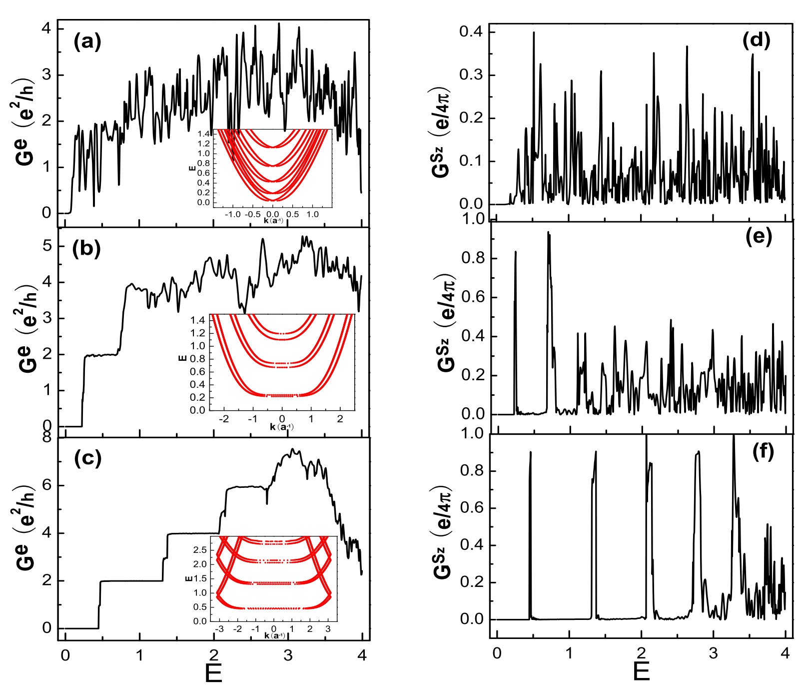

Figure 6